

Apparent Visible Wavelength

VERSION **v1.1**

RELEASE DATE **Sep 10th, 2024**

KEYWORDS **OCEAN COLOR**

Under: EARTH SCIENCE > OCEANS > OCEAN OPTICS

OCEAN OPTICS

Under: EARTH SCIENCE > OCEANS

WATER QUALITY INDEXES

Under: EARTH SCIENCE > TERRESTRIAL HYDROSPHERE > WATER QUALITY/WATER CHEMISTRY

CREATORS **Ryan Vandermeulen and Ivona Cetinic**

EDITORS **Guoqing Wang**

DOI **[10.5067/KAROCHG01RYJ](https://doi.org/10.5067/KAROCHG01RYJ)** 

Table of Contents

Abstract

Plain Language Summary

1. Introduction

2. Context / Background

2.1. Historical Perspective

2.2. Additional information

3. Algorithm Description

3.1. Scientific Theory

3.1.1. Assumptions

3.2. Mathematical Theory

3.2.1. Assumptions

3.3. Algorithm Input Variables

3.4. Algorithm Output Variables

4. Algorithm Availability

5. Algorithm Usage Constraints

6. Performance Assessment Validation

6.1. Performance Assessment Validation Methods

6.2. Performance Assessment Validation Uncertainties

6.3. Performance Assessment Validation Errors

7. Data Access

7.1. Input Data Data Access

7.1.1. Entry #1

7.2. Output Data Data Access

7.3. Important Related URLs

8. Contacts

References

Abstract

The Apparent Visible Wavelength (AVW) algorithm returns the weighted harmonic mean of the visible-range (400 – 700 nm) remote sensing reflectance (R_{rs}) wavelengths, in units of nanometers. The AVW is an optical water classification index, representing a one-dimensional geophysical metric that is inherently correlated to R_{rs} spectral shape (Vandermeulen et al. 2020). Since the entire visible-range spectrum is utilized in the calculation of AVW, this product ensures that any diagnostic signals present in the R_{rs} signal are considered, and affords the opportunity to describe and analyze spectral trends in R_{rs} in terms of a single variable. It is optimized for use on the entire suite of ocean color sensors (with sensor specific correction coefficients for multispectral sensors).

Plain Language Summary

Apparent Visible Wavelength (AVW) is a simplistic spectral classification derived from satellite-based ocean color information. Changing values equate to a change in the ocean's color, with lower values representing more clear water and higher values representing more turbid water. This tool is useful as it draws information from all available channels of ocean color instruments, and allows for visualisation and monitoring of small changes in highly complex data. It has been adapted across all the ocean color instruments, to allow for continuity and long term monitoring of the aquatic ecosystems.

1. Introduction

This algorithm returns the weighted harmonic mean of the visible-range (400 – 700 nm) remote sensing reflectance (R_{rs}) wavelengths, outputting the Apparent Visible Wavelength (AVW) in units of nanometers. The AVW is an optical water classification index, representing a one-dimensional geophysical metric that is inherently correlated to R_{rs} spectral shape (Vandermeulen et al. 2020). Since the entire visible-range spectrum is utilized in the calculation of AVW, this product ensures that any diagnostic signals present in the R_{rs} signal are considered, and affords the opportunity to describe and analyze spectral trends in R_{rs} in terms of a single variable.

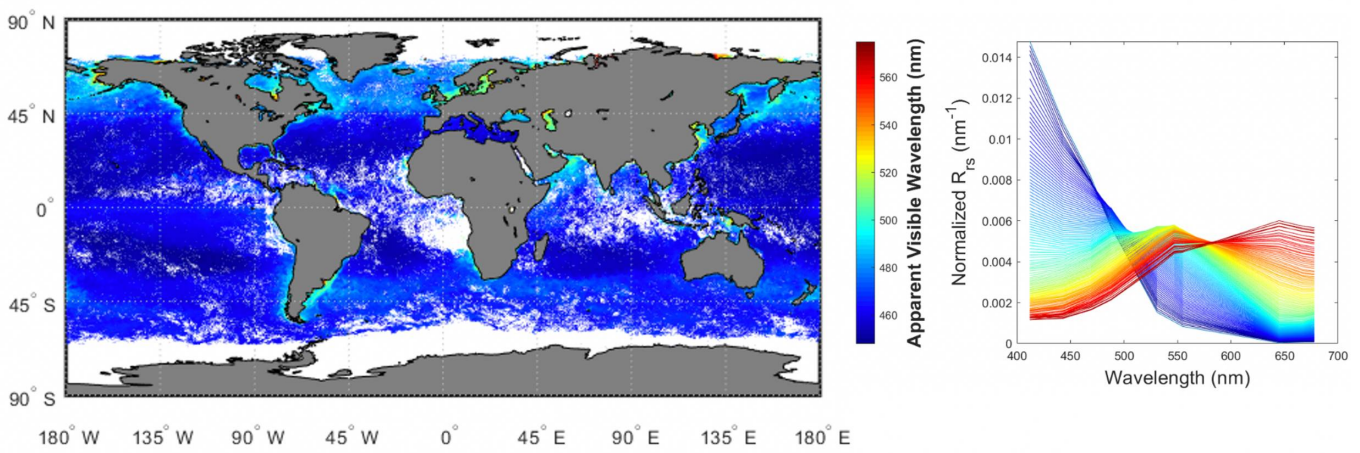


Figure 1: MODIS-Aqua AVW 32-day global composite (14Sep2018–15Oct2018), and the mean spectra (normalized to the numerical integration of R_{rs}) corresponding to the colormap.

2. Context / Background

2.1. Historical Perspective

Most of the algorithms used to derive geophysical parameters from satellites use only several wavelengths of available spectra, discarding potentially useful information that could allow for additional distinction of optical water types, ecosystem states, and similar. Spectral classification techniques, where full spectral $R_{rs}(\lambda)$ data are used to separate datasets into discrete classes based on spectral shape, have been used for years to address that issue. Approaches are highly diverse, but regardless of the methodology

used, many studies have demonstrated the value in using the full spectral information – especially when it comes to hyperspectral measurements of ocean color.

2.2. Additional information

No content available.

3. Algorithm Description

3.1. Scientific Theory

The derivation of the Apparent Visible Wavelength (AVW), at its most fundamental level, is simply a first-order measure of the dominant color of the water, as determined by the weight that each measured reflectance channel contributes to the albedo in the visible range of the spectrum. The output is not in the form of discrete classes, but instead a continuous gradient of wavelength values that represent a quantitative descriptor of weighted mean color reflected from the water's surface. At any point on this gradient, we find similarly shaped $R_{rs}(\lambda)$ spectra represented by the same AVW number.

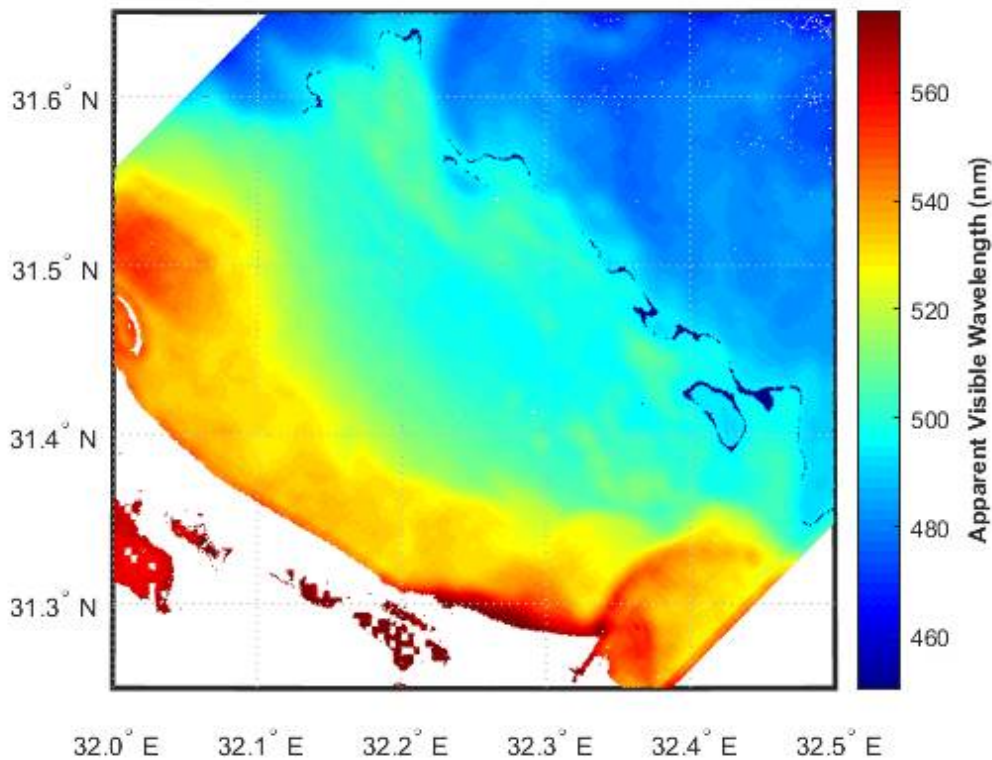


Figure 2: Here, the AVW is determined for an image obtained from the Hyperspectral Imager for the Coastal Ocean (HICO; H2012236112610.L2_ISS_OC.nc).

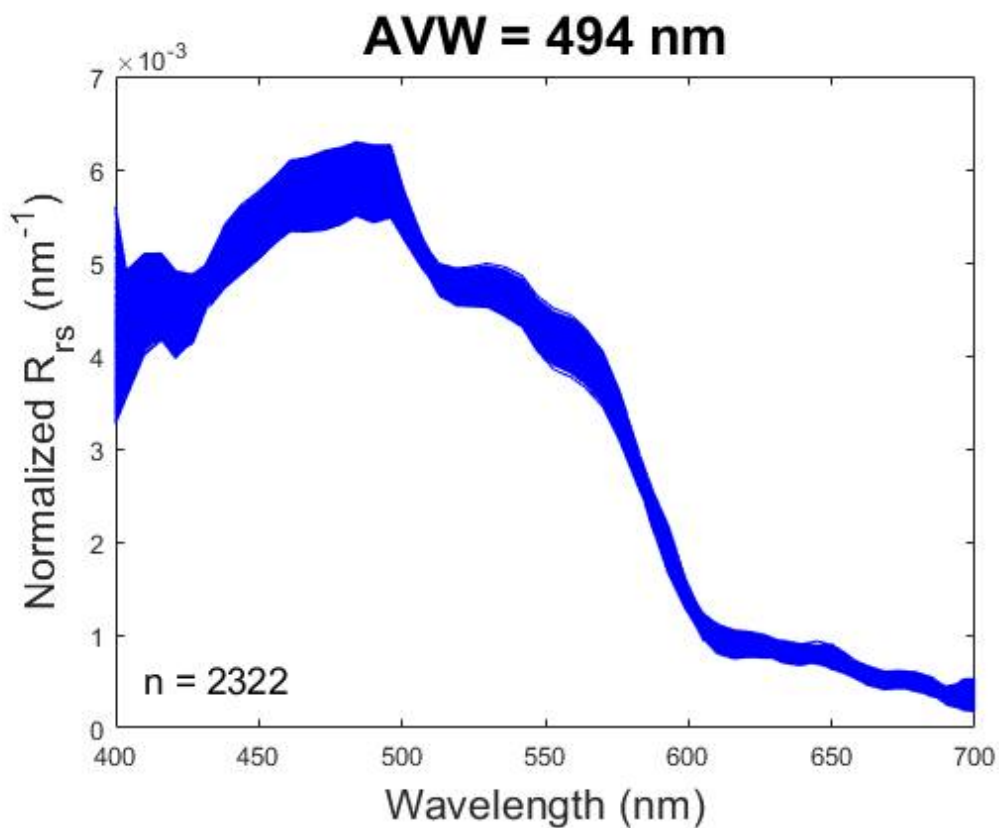


Figure 3: For the same scenes, all (normalized) R_{rs} spectra that fall within a moving window of AVW values are depicted. Incrementally stepping through a 40 nm range of AVW values reveals the spatial/spectral cohesion that makes AVW a useful optical water-type classification index.

3.1.1. Assumptions

No content available.

3.2. Mathematical Theory

The Apparent Visible Wavelength (AVW) is calculated as the weighted harmonic mean of all R_{rs} wavelengths, weighted as a function of the relative intensity of R_{rs} at each wavelength:

$$AVW = \frac{\sum_{\lambda_i=1}^{\lambda_n} R_{rs}(\lambda_i)}{\sum_{\lambda_i=1}^{\lambda_n} (R_{rs}(\lambda_i)/\lambda_i)} \quad (1)$$

To reconcile the impacts of spectral band placement on variance in spectral shape, an extensive in situ hyperspectral dataset Clark et al., 1997Bracher et al., 2015 Vandermeulen et al., 2017 is used to correlate sensors of varying multi- and hyperspectral resolutions, thereby promoting product continuity of the AVW between satellite sensors. $R_{rs}(\lambda)$ for each multispectral sensor are reconstructed from the 5,522 hyperspectral spectra, using the corresponding Relative Spectral Response (RSR) function for each satellite sensor. The hyperspectral AVW is compared to the multispectral AVW calculated for each sensor, and the coefficients from a polynomial fit are retained and applied to multispectral satellite data. Hyperspectral sensors undergo a slightly different procedure in I2gen. Since the multispectral coefficients are largely tuned with 1 nm spectral resolution data, hyperspectral satellite data are first interpolated to 1 nm spectral resolution using a spline interpolation function, and AVW is subsequently calculated without the use of a polynomial offset. With this correction, sensors with disparate spectral band placement (see table below) yield comparable AVW values to that of a hyperspectral sensor, further enabling an effective means of elucidating similarities or differences in spectral signatures within the constraints of two dimensions. See Vandermeulen et al. (2020) Vandermeulen et al., 2020 for details on a fit-for-purpose analysis performed on the AVW product multiple missions.

Table 1: Sensor-specific band centers used in AVW calculations.

Sensor	Sensor-specific band centers used in AVW calculations
--------	---

MODIS-Aqua	412, 443, 469, 488, 531, 547, 555, 645, 667, 678
MODIS-Terra	412, 443, 469, 488, 531, 547, 555, 645, 667, 678
OLCI-S3A	400, 412, 443, 490, 510, 560, 620, 665, 674, 682
OLCI-S3B	400, 412, 443, 490, 510, 560, 620, 665, 674, 681
MERIS	413, 443, 490, 510, 560, 620, 665, 681
SeaWiFS	412, 443, 490, 510, 555, 670
HawkEye	412, 447, 488, 510, 556, 670
OCTS	412, 443, 490, 516, 565, 667
GOCI	412, 443, 490, 555, 660, 680
VIIRS-SNPP	410, 443, 486, 551, 671
VIIRS-JPSS1	411, 445, 489, 556, 667
CZCS	443, 520, 550, 670
MSI-S2A	443, 490, 560, 665
MSI-S2B	443, 490, 559, 665
OLI	443, 482, 561, 655

Using the defined band centers (above) to calculate a sensor-specific AVW, the values are subsequently converted into a hyperspectral-equivalent AVW, using the following polynomial offsets:

Table 2: Sensor-specific polynomial coefficients used to calculate a sensor-specific AVW.

Sensor	c0, c1, c2, c3, c4, c5			
MODIS-Aqua	5.3223151E-09 1.7860303E+03	-1.3619239E-05 -1.8010144E+05	1.3886726E-02	-7.0534823E+00
MODIS-Terra	5.2820302E-09 1.7819361E+03	-1.3533547E-05 -1.7993575E+05	1.3817488E-02	-7.0277257E+00
OLCI-S3A	5.3756534E-10 1.9025240E+02	-1.3823300E-06 -1.9586876E+04	1.4217760E-03	-7.3259519E-01

OLCI-S3B	5.2874737E-10 1.8710170E+02	-1.3593836E-06 -1.9264929E+04	1.3979935E-03	-7.2032459E-01
MERIS	-1.8566476E-10 -1.2805555E+02	5.9630399E-07 1.4733655E+04	-7.3760077E-04	4.4214046E-01
SeaWiFS	1.3889225E-08 4.2173196E+03	-3.4666482E-05 -4.1487648E+05	3.4478423E-02	-1.7081781E+01
HawkEye	1.2484460E-08 3.8058444E+03	-3.1200493E-05 -3.7458936E+05	3.1064705E-02	-1.5404026E+01
OCTS	4.9443860E-09 1.6805142E+03	-1.2738386E-05 -1.6913709E+05	1.3043106E-02	-6.6374048E+00
GOCI	2.3513884E-10 1.0759457E+02	-6.3647535E-07 -1.2026274E+04	6.9347646E-04	-3.8202645E-01
SGLI	1.6912427E-09 8.4069664E+02	-4.9242779E-06 -9.0088850E+04	5.5741262E-03	-3.0863774E+00
VIIRS-SNPP	1.6399143E-09 5.2296625E+02	-4.1496452E-06 -5.2094618E+04	4.1742101E-03	-2.0901182E+00
VIIRS-JPSS1	3.8180817E-10 2.0172126E+02	-1.1345956E-06 -2.1958504E+04	1.2998933E-03	-7.2752517E-01
CZCS	2.5904658E-08 9.3033343E+03	-6.7326637E-05 -9.5665775E+05	6.9802590E-02	-3.6085795E+01
MSI-S2A	-7.4719643E-10 -2.3623942E+02	1.8794584E-06 2.3384674E+04	-1.8924228E-03	9.5069314E-01
MSI-S2B	-1.3572502E-09 -4.5046399E+02	3.4546589E-06 4.5327899E+04	-3.5159381E-03	1.7855878E+00
OLI	-7.5487887E-09 -2.4338650E+03	1.9136261E-05 2.4247497E+05	-1.9333568E-02	9.7261770E+00

A calibrated, hyperspectral "equivalent" AVW is then computed as:

$$AVW_{calibrated} = c0(AVW^5) + c1(AVW^4) + c2(AVW^3) + c3(AVW^2) + c4(AVW) + c5 \quad (2)$$

For PACE, all R_{rs} wavelengths from 400-700 nm range are used in calculation of AVW, and no offsets are applied (as OCI is already hyperspectral).

3.2.1. Assumptions

No content available.

3.3. Algorithm Input Variables

Name	Long Name	Unit
R_{rs}	Remote Sensing Reflectance	sr^{-1}

3.4. Algorithm Output Variables

Name	Long Name	Unit
avw	apparent visible wavelenght	nm

4. Algorithm Availability

No content available.

5. Algorithm Usage Constraints

Table 3: Algorithm implementation constrains.

Level-2 Product Suite	None (available through SeaDAS command-line processing)/PACE AOP suite
Level-3 Product Suite	avw (test product)
Calling in L2GEN	avw Note that each satellite will use its sensor-specific coefficients, to override the coefficients: <i>avw_coef = [c0, c1, c2, c3, c4, c5]</i>
Flags	PRODWARN - Pixels with negative Rrs values can adversely impact product viability. IF $Rrs_{vw} < 0$, PRODWARN is issued.

6. Performance Assessment Validation

6.1. Performance Assessment Validation Methods

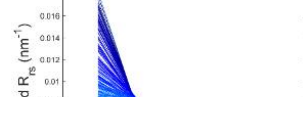
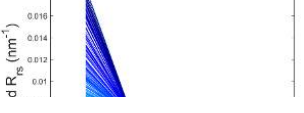
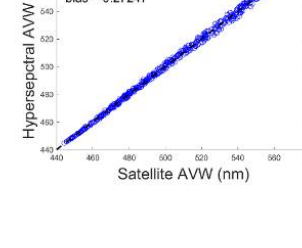
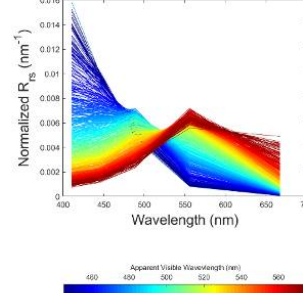
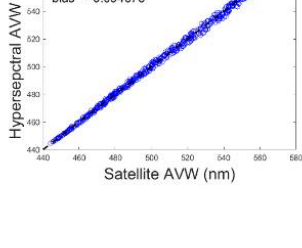
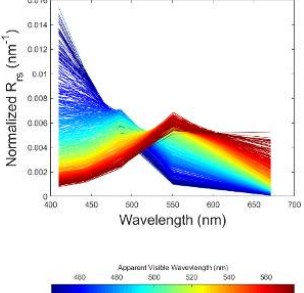
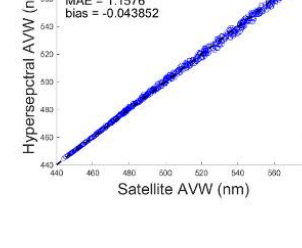
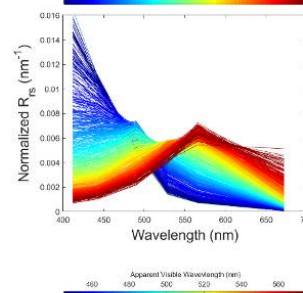
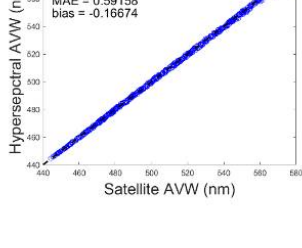
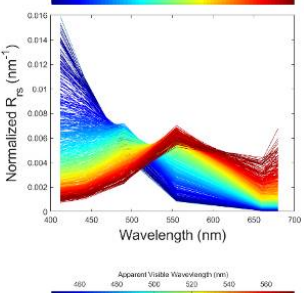
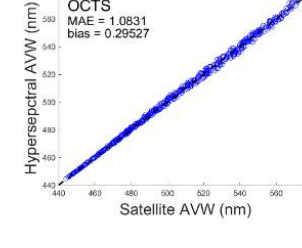
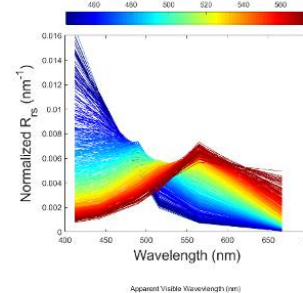
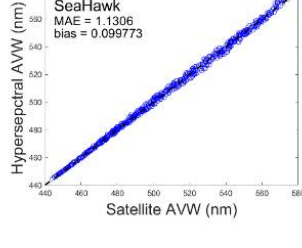
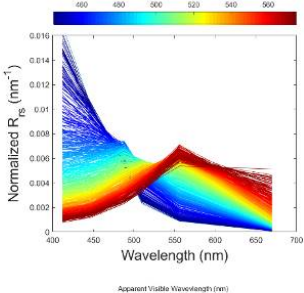
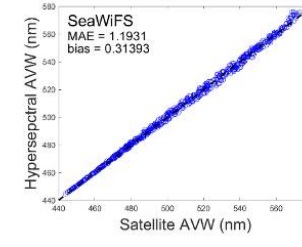
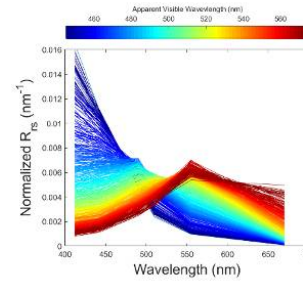
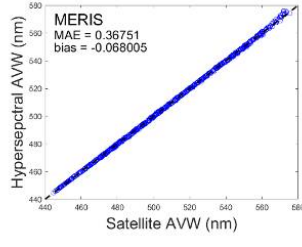
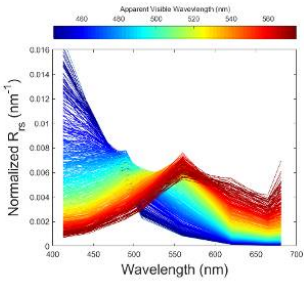
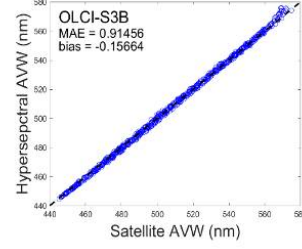
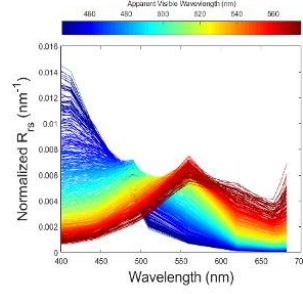
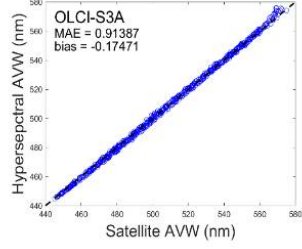
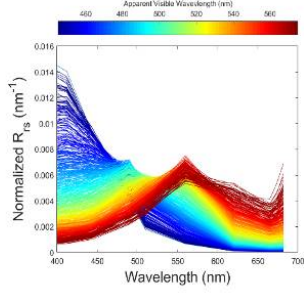
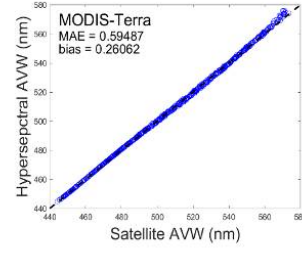
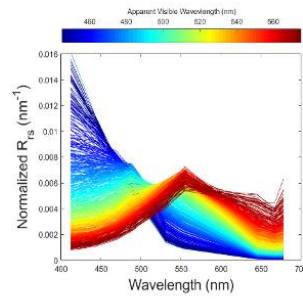
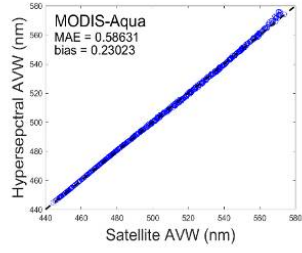
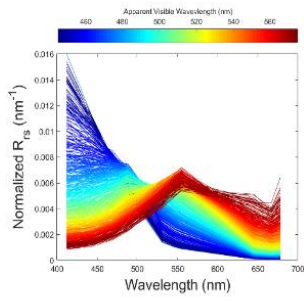
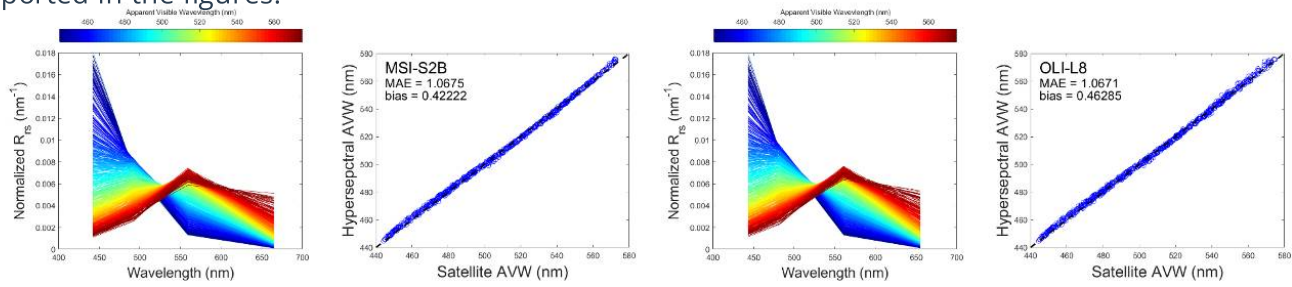


Figure 4: Independent assessment of polynomial validity using synthetic hyperspectral data (n = 624; Craig et al. 2020). The mean absolute error (MAE) and mean bias (Seegers et al. 2018) between true Hyperspectral AVW values and spectrally sub-sampled Hyperspectral-equivalent AVW values are reported in the figures.



6.2. Performance Assessment Validation Uncertainties

Uncertainties are not estimated for this product.

6.3. Performance Assessment Validation Errors

No content available.

7. Data Access

7.1. Input Data Data Access

7.1.1. Entry #1

URL	https://oceancolor.gsfc.nasa.gov/data/download_methods/
DESCRIPTION	The input Rrs at all available wavelengths between 400–700 nm (rrs_vvv) can be downloaded from the Ocean Color website using the various methods described in the provided link.

7.2. Output Data Data Access

No content available.

7.3. Important Related URLs

No content available.

8. Contacts

Ryan Vandermeulen

ROLES Writing – original draft, Writing – review & editing, Conceptualization, Methodology, Formal analysis & Software

AFFILIATIONS No affiliations in this document

EMAIL ryan.vandermeulen@noaa.gov

Ivona Cetinic

ROLES Data curation, Writing – review & editing, Validation & Corresponding Author

AFFILIATIONS No affiliations in this document

EMAIL ivona.cetinic@nasa.gov

URL <https://science.gsfc.nasa.gov/sed/bio/ivona.cetinic>

UUID <https://orcid.org/0000-0002-1363-3136>

References

- Bracher, A., Taylor, M. H., Taylor, B. B., Dinter, T., Rottgers, R. u. & Steinmetz, F. (2015). Phytoplankton pigments, hyperspectral downwelling irradiance and remote sensing reflectance during POLARSTERN cruises ANT-XXIII/1, ANT-XXIV/1, ANT-XXIV/4, ANT-XXVI/4, and Maria S. Merian cruise MSM18/3. <https://doi.org/10.1594/PANGAEA.847820>
- Clark, D. K., Gordon, H. R., Voss, K. J., Ge, Y., Broenkow, W. & Trees, C. (1997). Validation of atmospheric correction over the oceans. *Journal of Geophysical Research: Atmospheres*, *102(D14)*, 17209--17217. <https://doi.org/10.1029/96JD03345>
- Vandermeulen, R. A., Mannino, A., Craig, S. E. & Werdell, P. J. (2020). 150 shades of green: Using the full spectrum of remote sensing reflectance to elucidate color shifts in the ocean. *Remote Sensing of Environment*, *247*, 111900. <https://doi.org/10.1016/j.rse.2020.111900>
- Vandermeulen, R. A., Mannino, A., Neeley, A., Werdell, J. & Arnone, R. (2017). Determining the optimal spectral sampling frequency and uncertainty thresholds for hyperspectral remote sensing of ocean color. *Opt. Express*, *25(16)*, A785--A797. <https://doi.org/10.1364/OE.25.00A785>